

Exploiting Watermark-Based Defense Mechanisms in Text-to-Image Diffusion Models for Unauthorized Data Usage

Soumil Datta, Shih-Chieh Dai, Leo Yu, Guanhong Tao

University of Utah
Salt Lake City, UT

{soumil.datta, shihchieh.dai, zhuoxi.yu, guanhong.tao}@utah.edu

Abstract

Text-to-image diffusion models, such as Stable Diffusion, have shown exceptional potential in generating high-quality images. However, recent studies highlight concerns over the use of unauthorized data in training these models, which may lead to intellectual property infringement or privacy violations. A promising approach to mitigate these issues is to apply a watermark to images and subsequently check if generative models reproduce similar watermark features. In this paper, we examine the robustness of various watermark-based protection methods applied to text-to-image models. We observe that common image transformations are ineffective at removing the watermark effect. Therefore, we propose RATTAN, that leverages the diffusion process to conduct controlled image generation on the protected input, preserving the high-level features of the input while ignoring the low-level details utilized by watermarks. A small number of generated images are then used to fine-tune protected models. Our experiments on three datasets and 140 text-to-image diffusion models reveal that existing state-of-the-art protections are not robust against RATTAN.

1. Introduction

In the rapidly evolving landscape of artificial intelligence (AI), generative AI has emerged as one of the most transformative areas [24], with Text-to-Image (T2I) models such as Stable Diffusion [43] and DALL-E [42] gaining popularity. These models have made significant strides in generating highly realistic images [9, 36, 56], sometimes to the extent that even humans struggle to distinguish AI-generated content from actual photographs [4, 51]. Advancements in these models offer substantial benefits, including enhanced creative flexibility [17, 54] and a reduction in manual effort [15, 26, 41].

The success of these T2I models relies heavily on the large amounts of data available for training. For example,

widely used datasets, such as the LAION dataset, contain more than 5 billion image-text pairs [46]. However, these datasets may also include images that are intellectual property or private, which might be unintentionally incorporated into the model or even intentionally exploited by an adversary [1, 30, 30, 50]. For instance, an attacker might maliciously collect artwork from an artist without proper permission and train a T2I model on these samples. Once trained, the attacker could sell the generated images, which would be visually similar to the original artworks [8, 18]. This significantly raises concerns regarding unauthorized data usage, as it leads to intellectual property infringement or privacy violations [3, 59].

To address this problem, existing research has introduced various detection and protection approaches. Membership inference attacks [6, 33, 49] were originally designed to extract private information from a machine learning model by determining whether a given private input was part of its training data. These techniques can also be adapted to detect unauthorized data usage, as they share a similar goal [14, 25, 37]. However, it has been shown that membership inference attacks are less effective for T2I diffusion models [13], achieving only around a 66% detection rate on Stable Diffusion v1.5 [43].

Another line of research leverages a watermark as a secret key to modify protected images [11, 27, 32, 57]. Any T2I models trained on these samples will also “memorize” the watermark. During inference, the T2I model will generate images containing the watermark, which can thus be successfully detected. DIAGNOSIS [53], a state-of-the-art watermark-based protection method, applies a stealthy coating to protected images using a specialized function. Models trained on these coated images will produce outputs with a similar coating effect, thereby flagging the use of unauthorized data. Note that other watermarking methods aim to watermark AI-generated images [22, 31, 44, 60]. These methods differ from the focus of this paper, as they are applied to images already generated by models and aim to identify AI-generated content. In contrast, our work fo-

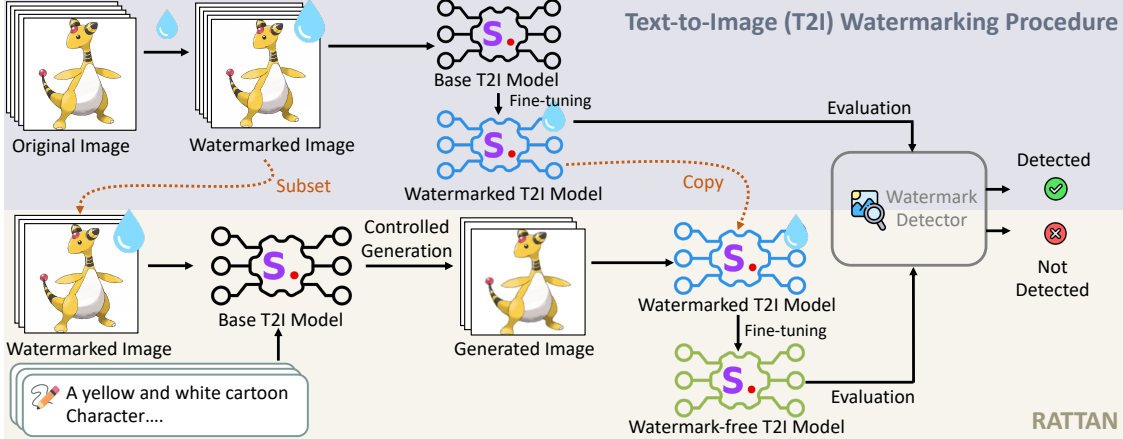


Figure 1. The top part represents the existing watermarking procedure for text-to-image diffusion models. The bottom part illustrates our method, RATTAN, for bypassing watermark-based protections. The text-to-image diffusion models shown in **black**, **blue**, and **green**, denote the **off-the-shelf base**, **watermarked**, and **watermark-free** versions, respectively.

cuses on preventing unauthorized data usage in T2I diffusion models, where the images in question are real (not AI-generated) and need protection from being illegitimately learned by such models.

In this paper, we investigate the robustness of state-of-the-art watermarking frameworks for T2I diffusion models. Specifically, we apply a set of common image transformations to watermarked images and observe that these transformations are largely ineffective at removing the watermark effect. This is due to the design of these approaches, which aim to preserve the fine-grained details of inputs – precisely the space utilized by watermarks. However, the primary goal of training on protected data is to generate images with similar high-level features. Hence, we propose to extract high-level coarse-grained features from protected images while ignoring low-level details. Particularly, we introduce RATTAN (**R**emoving **W**atermarks in **T**ext-to-**I**mage **A**ddition **N**etworks), which applies a controlled image generation process to protected images. The bottom part of Figure 1 illustrates the pipeline of RATTAN. Specifically, we leverage an off-the-shelf T2I model to generate a new version of the input based on both the protected image and the corresponding text. RATTAN takes advantage of the diffusion process to preserve key input features while removing unnecessary low-level details. The generated images are then used to fine-tune the model. Our evaluation on three datasets and 140 text-to-image diffusion models demonstrates that RATTAN can significantly reduce the detection rate of existing protections to 50%, equivalent to random guessing.

2. Background and Related Work

2.1. Text-to-Image Diffusion Model

Text-to-image diffusion models have gained popularity for their ability to generate high-quality images from textual descriptions [12, 45, 58]. Stable Diffusion [43], like other models, is an open-source generative model that iteratively transforms noisy data into coherent images through a diffusion process, producing highly detailed and diverse outputs [23, 38].

The diffusion process can be intuitively understood as a procedure of sequentially adding and removing Gaussian noise. Starting with an input image, random noise sampled from a normal distribution is iteratively added until the image is transformed into pure Gaussian noise. The goal of training a diffusion model is to learn a neural network that reverses this process, iteratively removing noise until the original input is recovered [5, 10, 55]. Formally, in the forward process of adding noise, given an initial input x^0 , its value at time step t is:

$$x^t = \alpha^t \cdot x^0 + \sigma^t \cdot z, z \sim \mathcal{N}(\mathbf{0}, \mathbf{I}), \quad (1)$$

where α^t is a constant derived from t that denotes the magnitude of x^t , and σ^t is a constant derived from t that determines the magnitude of noise z added to the image. The noise z is sampled from a standard normal distribution. The training objective of diffusion models is, therefore, to minimize the difference between the initial input x^0 and the denoised output obtained from x^t after processing it through the model multiple times.

$$\min_{\theta} \|\hat{x}^{t-1} - x^0\|_2^2, \quad (2)$$

$$\hat{x}^{t-1} = \hat{x}^t + \epsilon^2 \cdot f_{\theta}(\hat{x}^t, t) + \epsilon \cdot z, \quad (3)$$

where \hat{x}^t starts from x^t . Here, ϵ is a constant derived from σ , and f_θ represents the diffusion model, which takes the input \hat{x}^t and the current denoising time step t .

Stable Diffusion incorporates information extracted from text into the denoising process. Specifically, f_θ takes an additional feature vector representing the text features, allowing it to generate images that align with the descriptions provided in the input text.

However, training these models from scratch requires substantial computational resources. Consequently, most research focuses on fine-tuning pre-trained models [16, 35, 48], enabling them to adapt to specific tasks or datasets with a fraction of the computational power otherwise required.

2.2. Detecting Unauthorized Data Usage

Numerous research efforts have focused on detecting the use of unauthorized data in training and on mitigating models' tendencies to memorize sensitive or copyrighted information. Membership inference attacks [13, 19] are a feasible method to potentially determine if models have memorized data from the training set. Other defense mechanisms [28, 47, 52] introduced perturbations to images so that the model would be unable to learn specific features or styles from the image, thus preventing it from reproducing the image later. Similarly, backdoor watermarking techniques perturb the input training set with a watermark, such as injected steganography-based approaches that can embed binary strings into the image [32, 57], or backdoor image-transformation-based methods [53], so the model can learn and produce the watermark in its generated images. DIAGNOSIS [53] is a state-of-the-art watermark-based protection against unauthorized data usage in text-to-image diffusion models. It considers two watermark scenarios: the unconditional watermark, where the watermark is always present regardless of the text prompt, and the trigger-conditioned watermark, which appears only when a specific trigger sequence is included in the prompt.

3. Threat Model

In this work, we focus on evaluating the performance of watermark-based protections against unauthorized data usage in text-to-image diffusion models. This scenario involves two parties: the data owner or a third-party data protector, who acts as the defender, and the unauthorized model developer, who is the adversary.

Data Owner or Third-Party Data Protector (Defender).

The defender's goal is to prevent unauthorized usage or abuse of specific images that are either intellectual property or private. To achieve this, the data owner or a third-party data protector can intentionally embed imperceptible watermarks in these images, which serve as a secret key known only to the defender. Once text-to-image diffusion mod-

els are trained on such watermarked data, they will generate images containing the watermark. Thus, the defender's goal is to *detect whether a given model has been trained on unauthorized data* by inspecting its generated images. The data owner or protector has full access to the protected data but not to other training data used by the diffusion model. They do not have access to the model itself or the training process and can only query the trained model to obtain generated images. This setup simulates scenarios involving model API providers, such as Midjourney [2].

Unauthorized Model Developer (Adversary). The adversary, or unauthorized model developer, aims to use protected images to train their text-to-image diffusion model so that it can generate similar images or images with specific features. However, the adversary wants to avoid the detection of unauthorized data usage in their trained model. To achieve this, they may first clean the training data, such as applying image transformations, before using it to train the text-to-image model. They might also inspect or modify the model post-training to remove any embedded watermarks. The adversary does not know whether or which images contain watermarks, nor do they have access to the watermark detector developed by the defender to determine if the model has been trained on unauthorized data.

4. Method

The main characteristic of watermark-based protections is that the added coatings or perturbations are visually imperceptible. This ensures that the watermark, or "secret key," is known only to the data owner and remains hidden from data consumers, such as text-to-image model developers. Given this, our goal is to evaluate the robustness of these watermarks – for example, to determine if they can be removed or degraded by various image transformations.

4.1. Image Transformation

Since watermark-based protections add small perturbations to protected images, a straightforward approach to evaluate their robustness is to apply various image transformations to these images. We leverage three commonly used transformation methods: Gaussian blur, JPEG compression, and color jittering. Figure 2 shows the images after applying the aforementioned transformation methods. The second column presents the image embedded with the DIAGNOSIS watermark, which is an image-warping function that distorts straight lines into curly ones, as illustrated in image (b) compared to the original image (a). After applying the different transformations, it can be observed that the boundary lines remain curly, indicating that the watermark effect persists. We further evaluate six other image transformations in Section 5.3 and reach the same conclusion.

Image transformations fail to remove the watermark effect because they cannot significantly alter the input image



Figure 2. Comparison of (a) the original image, (b) DIAGNOSIS watermarked image, and the images after applying (c) Color Jittering, (d) Gaussian Blur, (e) JPEG Compression. The bottom row provides a zoomed-in view. The curly-line characteristic of the watermark is still visible in each transformed image. (f) presents the result after RATTAN’s controlled image generation on the watermarked input. The lines appear smoother compared to the original image.

(to preserve the primary content). These watermarks are designed to be robust against common distortions. For instance, an attacker might photograph a piece of art on display and use that image for model training. The watermark should persist despite adjustments in lighting, contrast, noise, and other minor variations. Consequently, simple image transformations cannot effectively eliminate the watermark effect. However, this does not imply that existing protections are immune to all possible manipulations. In the following section, we demonstrate how our new design can bypass these protections.

4.2. Our Solution

The primary function of text-to-image models is to generate images that align with input text descriptions. When unauthorized data is used in training, the model’s capability extends to generating images with features similar to those in the protected images. Existing watermark-based protections assume that for a model to generate similar images, it must be trained on the exact content of the protected images. This process would lead to the watermark being embedded into the model. However, this assumption does not always hold. As long as the model learns the key features of the protected data, it can generate similar images without directly replicating the original content (e.g., the watermark).

We propose to leverage the generative capabilities of diffusion models to construct data samples that share key features with protected images. Instead of directly using the protected images in training, we employ a technique similar to zero-shot learning. Here, a diffusion model is prompted to generate an image based on a text description along with a reference (protected) image. In this way, the diffusion model has the freedom to create images without focusing on details such as the watermark embedded in the protected images.

Figure 1 presents an overview of our method, RATTAN,

for bypassing watermark-based protections. The top part of the figure illustrates how existing watermark-based protection methods operate, which involve two steps. The first step is embedding a watermark onto protected images. This watermark can be either a sequence of pixel value bits or an image transformation function. The second step involves inspecting the generated images from text-to-image diffusion models. If the model has been trained on watermarked data, the generated images will also contain this watermark. Consequently, existing protections can flag the trained model.

The bottom part of Figure 1 shows the pipeline of our technique, RATTAN. The adversary’s goal is to train a text-to-image model on unauthorized data. Without knowing whether these protected images are watermarked, RATTAN selects a subset of the data (e.g., 10 images) and their corresponding text descriptions. It then employs an off-the-shelf Stable Diffusion [43] model to perform controlled image generation based on both the input image and its corresponding text. The generated images are intended to retain the high-level key features of the protected data but be free of watermarks. RATTAN then uses this small set of images to fine-tune the potentially watermarked text-to-image model. Below, we detail the two main components of RATTAN: controlled image generation and watermark removal.

Controlled Image Generation. As discussed above, our goal is to obtain images that preserve key features of protected data without copying the fine-grained details used by watermarks. Our idea is to leverage an off-the-shelf diffusion model to perform controlled image generation. Specifically, the model has a certain freedom to create an image based on the given text and the protected input.

For diffusion models, the generation process typically starts from random Gaussian noise, as described in Equation 3, and then iteratively removes the noise by passing it through the model. In our scenario, we aim to generate an

image that retains the major features of the protected input, such as structures and outlines. To achieve this, similar to existing work [34], rather than starting the generation process from random Gaussian noise, RATTAN uses a starting point obtained from the protected image.

Specifically, given the projected image $x_{protected}$, we first apply [Equation 1](#) to it, which essentially adds random noise to the image.

$$x_{guide}^t = \alpha^t \cdot x_{guide}^{t-1} + \sigma^t \cdot z, z \sim \mathcal{N}(\mathbf{0}, \mathbf{I}), \quad (4)$$

$$x_{guide}^0 = x_{protected} \quad (5)$$

In the standard diffusion process, the output from the above equations after t iterations becomes Gaussian noise, and the diffusion model aims to recover the original input. This is why, after training, the diffusion model can generate images from random noise. Here, our goal is to preserve the key high-level features of the protected input, such as structures, outlines, color schemes, etc., so that the diffusion model can recover these coarse features while filling in fine-grained details. Thus, we do not add noise to $x_{protected}$ until it becomes Gaussian noise but rather stop at a certain step. Suppose the total number of iterations needed to transform an image to random noise is t ; our diffusion process ([Equation 4](#)) only applies for $\gamma \cdot t$ iterations. Empirically, we choose $\gamma = 0.6$ as it provides the best trade-off between the quality of generated images and the evasion rate. The results of using different γ values are discussed in [Section 5.5](#).

After obtaining the diffused $x_{protected}$, i.e., x_{guide} , we pass it through a standard diffusion model to generate a new image, as illustrated in [Equation 3](#). Note that we use an off-the-shelf diffusion model (not the model trained on the protected data) in RATTAN, with its weight parameters frozen.

In addition to the original protected image, we also include its paired text description as a reference. This is because the final text-to-image model is trained on both the image and the text, with the text providing guidance on which parts the model should focus on during training. Thus, we leverage the text in our controlled image generation as well. This approach follows the standard Stable Diffusion [43] inference process, where the text embedding from a text encoder is incorporated into the cross-attention layers during the denoising process. More details can be found in the original paper [43].

The last column (f) in [Figure 2](#) shows the result after applying RATTAN to the watermarked input (b). Observe that the generated image has smooth boundary lines, effectively removing the watermark effect present in (b). Additionally, the Pokémon’s teeth are no longer visible, and the color tone differs from the original image. This is due to the controlled generation process, which preserves high-level features while disregarding low-level details.

Watermark Removal. Since our generated images from protected inputs do not contain watermarks, a straightfor-

ward approach is to apply controlled image generation to all the training data. However, there are two issues with this method. First, the training set could be extensively large, and applying the diffusion model generation to all samples can be computationally expensive and substantially increase costs. Second, as discussed earlier, the controlled generation retains the key high-level features of protected images while ignoring low-level details. Although this helps to eliminate watermarks, it also removes fine-grained features necessary for training text-to-image models.

The watermarked model has already been trained on protected images with fine-grained details, including the watermark. We only need to remove the watermark without affecting the fine-grained content features. To achieve this, we propose to fine-tune the watermarked model on a small set of our generated images. Note that the text-to-image model is trained on text-image pairs. The original watermarked model has learned the correspondence between the text and the watermarked image. We use the same text but pair it with our generated image – a slightly different version of the protected image. This guides the model to ignore the watermark and focus on the main content features, both coarse-grained and fine-grained. Our evaluation in [Section 5.2](#) shows that with as few as 10 images, RATTAN can effectively eliminate the watermark effect.

5. Evaluation

This section discusses the evaluation on RATTAN and a few image transformations, as well as ablations studies to understand the impact of different components in RATTAN.

5.1. Experimental Setup

Datasets. We utilize three popular datasets: Pokemon [40] (833 text-image pairs), Naruto [7] (1221 text-image pairs), and CelebA [29]. For the CelebA dataset, we use the first 1000 text-image pairs to be consistent with the experimental setting in the DIAGNOSIS paper.

Watermarking Methods. We use three watermark-based protection methods for evaluation, namely the works by Luo *et al.* [32], Yu *et al.* [57], and DIAGNOSIS [53]. Luo *et al.* and Yu *et al.* employ a bit string as the watermark and DIAGNOSIS uses a warping function. DIAGNOSIS supports both unconditional and trigger-conditioned watermarks. In the unconditional setting, the watermark is activated for any text prompt. In the trigger-conditioned setting, the watermark appears only when the prompt contains a specific text trigger or a predefined token sequence at the beginning.

Models and Fine-tuning. We primarily use Stable Diffusion v1.4 [43] along with the Low-Rank Adaptation of Large Language Models (LoRA) fine-tuning method [21] for our experiments. The evaluation on other diffusion mod-

Table 1. Detection results of different watermark-based protections before and after applying RATTAN.

Watermark	Method	TP	TN	FP	FN	Acc.
Luo <i>et al.</i> [32]	Original	0	5	0	5	50%
	RATTAN	0	5	0	5	50%
Yu <i>et al.</i> [57]	Original	0	5	0	5	50%
	RATTAN	0	5	0	5	50%
DIAGNOSIS [53]	Original	5	5	0	0	100%
	RATTAN	0	5	0	5	50%

els is presented in the supplementary. We also include ablation studies with different Stable Diffusion models for controlled generation in the RATTAN pipeline in Section 5.5. For each experiment, we train 10 models for both clean and watermarked models to minimize the randomness.

Metrics. We make use of several metrics to evaluate the results. For the detection on unauthorized data usage, we use True Positives (malicious models detected as malicious), True Negatives (benign models detected as benign), False Positives (benign models detected as malicious), and False Negatives (malicious models detected as benign). For example, the goal of RATTAN is to shift the results of True Positives towards False Negatives, i.e., allow malicious models with unauthorized data usage to be considered benign. We also calculate the average of Fréchet Inception Distance (FID) [20] of the generated images from each model to measure the generation quality, as well as report on the model’s memorization strength to determine how close it is to being detected as malicious.

5.2. Evading Watermark-based Protections

In this section, we evaluate the performance of RATTAN on the works by Luo *et al.* [32], Yu *et al.* [57], and DIAGNOSIS [53]. Table 1 shows the results on the Pokemon dataset. For each watermarking method, we trained 10 models: 5 models with the watermark in the training set and 5 benign models where the training set is unmodified. As shown in the table, the watermarks implemented by Luo *et al.* and Yu *et al.* are not effectively memorized by the diffusion model, making them unreliable for detecting malicious behavior. Luo *et al.* and Yu *et al.*’s methods implement fingerprinting of images using binary strings, with detection conducted by measuring the bit accuracy of generated samples. The average bit accuracy for raw images (images with the watermark directly added) produced by Luo *et al.* was approximately 68.11%, while for Yu *et al.*, it was around 46.93%. This demonstrates the limited effectiveness of these methods in embedding watermarks. In contrast, DIAGNOSIS performs significantly better, with a 100% detection accuracy. However, for all three watermarking methods, RATTAN successfully reduces their detection accuracy to 50%, equivalent to

random guessing.

Results on DIAGNOSIS. As observed above, since the other two watermarking methods result in poor memorization of watermarks in diffusion models, we mainly focus on DIAGNOSIS in the following evaluation.

For our experiments, we adopt a similar setting to the one used in the DIAGNOSIS paper. We use 50 different text prompts to generate images from the fine-tuned models and report the FID scores and memorization strengths. We train 20 models for each case: 10 models using unauthorized data and 10 models without unauthorized data. Our goal is to shift True Positives towards False Negatives, achieving an overall accuracy of 50%, equivalent to random guessing. Table 2 presents the evaluation results.

Observe that DIAGNOSIS performs well on most datasets, with high accuracy and memorization strengths. However, RATTAN can successfully shift the true positives towards false negatives, yielding a 50% detection accuracy by DIAGNOSIS, which is equivalent to random guessing. The memorization is significantly reduced from nearly 1 to 0.3 in most cases. Additionally, the FID scores of the models after applying RATTAN are similar or even lower than those of DIAGNOSIS-watermarked models. This demonstrates that RATTAN can effectively preserve the normal functionality of T2I models while removing watermarks.

5.3. Performance of Image Transformations

As discussed in Section 4.1, one straightforward idea to remove watermarks is to apply image transformations. We have shown earlier that Gaussian blur, JPEG compression, and color jittering cannot remove the watermark embedded by DIAGNOSIS. Here, we evaluate six more image transformations, including saturation increase, using 8-bit quantization, adding a green hue, increasing the contrast, cropping by a factor of 1.5 on each side, and increasing the brightness. The results are shown in Table 3.

From the table, we observe that DIAGNOSIS is highly effective against most image transformations. However, its performance declines when contrast is increased in the training set. The strong performance of DIAGNOSIS against popular image transformation-based mitigation strategies underscores the need for RATTAN to provide a more robust evaluation.

5.4. Visualization of RATTAN Generated Images

Figure 2 illustrates the image generated by RATTAN based on the protected input. The bottom row provides a zoomed-in view of a specific region of the image. The first column shows the original image before undergoing DIAGNOSIS’s watermarking process. In the second column, DIAGNOSIS applies a watermark, noticeable as slight wobbliness along the edges. This edge perturbation introduces a feature that can be subtly learned by the diffusion model while remain-

Table 2. Evaluation of RATTAN against DIAGNOSIS across various datasets.

Dataset	Method	Memorization Type	Metrics					FID ↓	Memorization ↓
			TP	TN	FP	FN	Acc		
Pokemon	Diagnosis	Unconditional	10	10	0	0	100%	214.86 ± 9.02	0.830
		Trigger-Conditioned	10	10	0	0	100%	270.57 ± 11.61	1.000
	RATTAN	Unconditional	0	10	0	10	50%	211.59 ± 3.15	0.327
		Trigger-Conditioned	0	10	0	10	50%	214.09 ± 3.33	0.173
Naruto	Diagnosis	Unconditional	7	10	0	3	85%	240.13 ± 7.15	0.790
		Trigger-Conditioned	10	10	0	0	100%	257.67 ± 9.61	0.912
	RATTAN	Unconditional	0	10	0	10	50%	241.91 ± 6.77	0.360
		Trigger-Conditioned	0	10	0	10	50%	244.82 ± 10.98	0.246
CelebA	Diagnosis	Unconditional	10	10	0	0	100%	237.63 ± 6.33	0.996
		Trigger-Conditioned	10	10	0	0	100%	240.11 ± 8.99	1.000
	RATTAN	Unconditional	0	10	0	10	50%	230.52 ± 5.55	0.491
		Trigger-Conditioned	0	10	0	10	50%	232.66 ± 4.01	0.299

ing robust against most image transformations. The last column presents the result after RATTAN generates a new image based on the watermarked input and the corresponding text. RATTAN’s controlled image generation smooths out these added perturbations, effectively ignoring low-level details. Importantly, the generated image retains most of the essential features of the original image, ensuring the intellectual property quality remains unaffected.

5.5. Ablation Study

In this section, we present the results of our ablation study on the performance of RATTAN. First, we investigate how fine-tuning with different numbers of cleaned samples affects the efficacy of our method. Next, we examine the impact of varying the number of fine-tuning epochs. Finally, we evaluate the effectiveness of our approach across various diffusion models. Additionally, we consider training a model from scratch using RATTAN-generated images. The results of each ablation study on the Pokemon dataset are shown in Table 3. Since the protection method does not misclassify benign models (those not trained on unauthorized data) as malicious, we only report the detection rate for watermarked models after applying RATTAN in Table 3.

Impact of RATTAN-Generated Samples. We first examine the effect of fine-tuning on different numbers of RATTAN-generated images, ranging from as few as 5 samples to the entire training set of 783 samples. The results in Table 3 indicate that fine-tuning with a smaller subset of cleaned samples results in relatively lower FID scores. This occurs because RATTAN-generated images primarily preserve high-level features while disregarding low-level details. Fine-tuning on a larger amount of such data may impact the model’s ability to generate high-quality images. On the other hand, using the full dataset results in a few malicious detections, suggesting that training on a larger num-

Table 3. Ablation study across several factors: the image transform method, the number of fine-tuning samples, the number of epochs, parameter γ , and the version of Stable Diffusion.

Ablation		FID ↓	Detection ↓	Memorization ↓
Image Transform	Saturation	229.80 ± 6.15	90%	0.874
	8-bit Quant.	223.30 ± 7.76	90%	0.860
	Hue Shift (Green)	243.14 ± 8.64	100%	0.896
	Contrast	234.51 ± 7.83	70%	0.718
	Cropped	234.68 ± 7.01	100%	0.852
	Brightness	232.24 ± 7.39	90%	0.840
# Sample	5	217.97 ± 6.81	0%	0.199
	10	214.27 ± 4.19	0%	0.253
	50	209.36 ± 4.34	0%	0.120
	200	210.76 ± 6.75	0%	0.132
	500	215.29 ± 7.38	0%	0.141
	783	234.62 ± 3.91	20%	0.640
# Epoch	5	214.66 ± 4.80	0%	0.336
	15	220.10 ± 7.26	0%	0.296
	30	220.53 ± 5.82	0%	0.284
	50	211.99 ± 5.82	0%	0.224
	100	214.24 ± 3.24	0%	0.168
	0.2	234.15 ± 11.77	80%	0.830
γ	0.4	226.29 ± 6.59	20%	0.560
	0.6	211.59 ± 3.15	0%	0.327
	0.8	218.95 ± 6.99	0%	0.518
	1.0	227.72 ± 5.56	50%	0.744
	SD v1.4	210.70 ± 8.65	0%	0.193
Model	SD v2.0	216.24 ± 6.40	0%	0.224
	SD v3 Medium	216.46 ± 6.38	0%	0.202

ber of samples might increase the risk of overfitting to the watermarked features.

Impact of Fine-tuning Epochs. In this experiment, we examine the impact of varying the fine-tuning epochs in the RATTAN pipeline. By testing a range of epochs from 5 to 100, we evaluate the trade-off between image quality, as measured by the FID score, and the degree of memorization. The results in Table 3 indicate that the number of fine-tuning epochs has a relatively minor impact on the FID score. However, memorization strength decreases signifi-

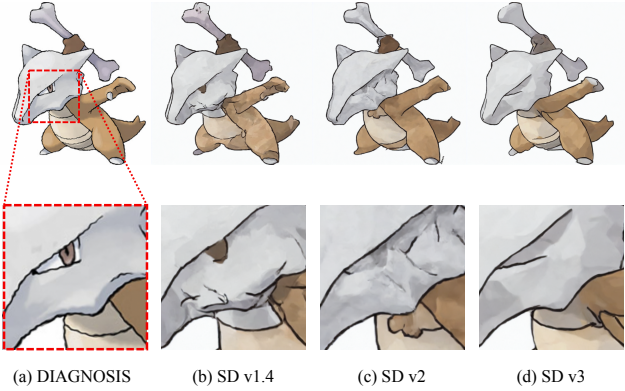


Figure 3. Comparison of images generated by different versions of Stable Diffusion.

antly as the number of epochs increases, dropping from 0.336 at 5 epochs to 0.168 at 100 epochs. This decline suggests that extended fine-tuning progressively reduces the retention of watermarked content, resulting in more effective watermark removal. However, it is worth noting that longer fine-tuning periods are computationally expensive. To achieve a balance between watermark removal efficacy and computational efficiency, RATTAN employs 30 epochs for fine-tuning.

Impact of γ . The parameter γ in the image generation pipeline controls the degree of transformation applied to the input image. Larger γ values place greater emphasis on the textual prompt, while smaller values result in outputs that closely align with the initial protected image. For larger γ values, the diffusion model introduces more noise to the input, allowing for greater divergence from the original protected image. As shown in Table 3, smaller γ values (e.g., 0.2) result in a high false negative rate, likely because the original image features are preserved sufficiently to retain the watermark. Conversely, the largest γ value tested (1.0) also shows an increased malicious detection rate. This is because the generated images diverge significantly from the original inputs, failing to preserve essential content. Such samples, when paired with the text, do not effectively guide the T2I models to disregard the learned watermark.

Impact of Diffusion Models on Controlled Image Generation. We evaluated the effectiveness of various Stable Diffusion models within the RATTAN pipeline during the controlled generation process. Each model processed watermarked images to minimize the visual artifacts introduced by the watermark. The results are summarized in Table 3 and visualized in Figure 3.

Our experiments show that Stable Diffusion (SD) v1.4 achieves the lowest average FID scores, indicating the closest alignment with the original data distribution, followed by SD v2.0 and SD v3 Medium. Across all models, the

detection rate is 0%, demonstrating that no detectable watermarks remain after fine-tuning on the cleaned images, regardless of the model version.

Figure 3 visualizes the controlled generation results across different models. Although the differences are subtle, SD v1.4 produces images that appear slightly closer to the original inputs. This ablation study suggests that SD v1.4 performs marginally better in both FID score and memorization reduction, making it a better choice for RATTAN when high fidelity to the original data is desired.

Training with RATTAN-Generated Images from Scratch. All the above experiments involve fine-tuning the watermarked model on RATTAN-generated images. Since RATTAN-generated images are already free of the watermark effect, an alternative approach is to directly train a model from scratch using all the generated images. However, the results show that the model trained in this manner has a high FID score of 269.64 and a detection rate of 10%. As discussed in Section 4.2, the controlled generation retains the key high-level features of protected images while ignoring low-level details. Although this helps to eliminate watermarks, it also removes fine-grained features necessary for training text-to-image models. Therefore, the trained model has a much higher FID score compared to fine-tuning on a small subset.

6. Conclusion

This paper investigates watermark-based protections against unauthorized data usage in text-to-image diffusion models. We find that common image transformations are largely ineffective at nullifying watermark effects. To address this, we propose RATTAN, a framework that effectively erases a model’s memorization of watermarks, rendering watermark-based protections non-robust. Our approach requires as few as 10 images to successfully remove watermarks across various datasets and protection methods. This work highlights the limitations of existing watermark-based techniques for intellectual property protection and underscores the need to develop more robust defense strategies.

Limitations. While RATTAN offers an intuitive approach to evaluate the robustness of watermark-based protections in diffusion models, there are certain limitations that need further investigation. First, the controlled generation process may not fully recover all original image features, which could lead to a slight degradation in image quality compared to the unaltered training data. Our results indicate that in most cases, RATTAN-trained models achieve FID scores comparable to those of the original models. Second, this paper primarily focuses on the issue of unauthorized data usage in text-to-image diffusion models. Similar challenges exist in large language models (LLMs), but it

is unclear whether RATTAN would be effective in this context. Since the design of RATTAN is general and relies only on an off-the-shelf model for controlled generation, it could potentially be adapted for LLMs. We leverage experimental exploration to future work.

References

- [1] Andersen v. stability ai ltd., 23-cv-00201-who. <https://www.courtlistener.com/docket/67656604/andersen-v-stability-ai-ltd/>, 2023. N.D. Cal., Oct. 30, 2023. [1](#)
- [2] Midjourney. <https://www.midjourney.com/home>, 2024. [3](#)
- [3] Oliver Bendel. Image synthesis from an ethical perspective. *AI & SOCIETY*, pages 1–10, 2023. [1](#)
- [4] Sergi D Bray, Shane D Johnson, and Bennett Kleinberg. Testing human ability to detect ‘deepfake’ images of human faces. *Journal of Cybersecurity*, 9(1):tyad011, 2023. [1](#)
- [5] Hanqun Cao, Cheng Tan, Zhangyang Gao, Yilun Xu, Guangyong Chen, Pheng-Ann Heng, and Stan Z Li. A survey on generative diffusion models. *IEEE Transactions on Knowledge and Data Engineering*, 2024. [2](#)
- [6] Nicolas Carlini, Jamie Hayes, Milad Nasr, Matthew Jagielski, Vikash Sehwag, Florian Tramer, Borja Balle, Daphne Ipolitio, and Eric Wallace. Extracting training data from diffusion models. In *32nd USENIX Security Symposium (USENIX Security 23)*, pages 5253–5270, 2023. [1](#)
- [7] Eole Cervenka. Naruto blip captions. <https://huggingface.co/datasets/lambdalabs/naruto-blip-captions/>, 2022. [5](#), [1](#)
- [8] Eva Cetinic and James She. Understanding and creating art with ai: Review and outlook. *ACM Transactions on Multimedia Computing, Communications, and Applications (TOMM)*, 18(2):1–22, 2022. [1](#)
- [9] Shin-I Cheng, Yu-Jie Chen, Wei-Chen Chiu, Hung-Yu Tseng, and Hsin-Ying Lee. Adaptively-realistic image generation from stroke and sketch with diffusion model. In *Proceedings of the IEEE/CVF Winter Conference on Applications of Computer Vision (WACV)*, pages 4054–4062, 2023. [1](#)
- [10] Florinel-Alin Croitoru, Vlad Hondru, Radu Tudor Ionescu, and Mubarak Shah. Diffusion models in vision: A survey. *IEEE Transactions on Pattern Analysis and Machine Intelligence*, 45(9):10850–10869, 2023. [2](#)
- [11] Yingqian Cui, Jie Ren, Han Xu, Pengfei He, Hui Liu, Lichao Sun, Yue Xing, and Jiliang Tang. Diffusionshield: A watermark for copyright protection against generative diffusion models. *arXiv preprint arXiv:2306.04642*, 2023. [1](#)
- [12] Prafulla Dhariwal and Alexander Nichol. Diffusion models beat gans on image synthesis. *Advances in Neural Information Processing Systems*, 34:8780–8794, 2021. [2](#)
- [13] Jinhao Duan, Fei Kong, Shiqi Wang, Xiaoshuang Shi, and Kaidi Xu. Are diffusion models vulnerable to membership inference attacks? In *International Conference on Machine Learning*, pages 8717–8730. PMLR, 2023. [1](#), [3](#)
- [14] Jan Dubiński, Antoni Kowalcuk, Stanisław Pawlak, Przemysław Rokita, Tomasz Trzciński, and Paweł Morawiecki. Towards more realistic membership inference attacks on large diffusion models. In *Proceedings of the IEEE/CVF Winter Conference on Applications of Computer Vision (WACV)*, pages 4860–4869, 2024. [1](#)
- [15] Alexander Dunkel, Dirk Burghardt, and Madalina Gugulica. Generative text-to-image diffusion for automated map production based on geosocial media data. *KN-Journal of Cartography and Geographic Information*, 74(1):3–15, 2024. [1](#)
- [16] Ying Fan, Olivia Watkins, Yuqing Du, Hao Liu, Moonkyung Ryu, Craig Boutilier, Pieter Abbeel, Mohammad Ghavamzadeh, Kangwook Lee, and Kimin Lee. Reinforcement learning for fine-tuning text-to-image diffusion models. *Advances in Neural Information Processing Systems*, 36, 2024. [3](#)
- [17] Ruoyu Feng, Wenming Weng, Yanhui Wang, Yuhui Yuan, Jianmin Bao, Chong Luo, Zhibo Chen, and Baining Guo. Credit: Creative and controllable video editing via diffusion models. In *Proceedings of the IEEE/CVF Conference on Computer Vision and Pattern Recognition*, pages 6712–6722, 2024. [1](#)
- [18] Jessica L Gillotte. Copyright infringement in ai-generated artworks. *UC Davis L. Rev.*, 53:2655, 2019. [1](#)
- [19] Jamie Hayes, Luca Melis, George Danezis, and Emiliano De Cristofaro. Logan: Membership inference attacks against generative models. *arXiv preprint arXiv:1705.07663*, 2017. [3](#)
- [20] Martin Heusel, Hubert Ramsauer, Thomas Unterthiner, Bernhard Nessler, and Sepp Hochreiter. Gans trained by a two time-scale update rule converge to a local nash equilibrium, 2018. [6](#)
- [21] Edward J Hu, Yelong Shen, Phillip Wallis, Zeyuan Allen-Zhu, Yuanzhi Li, Shean Wang, Lu Wang, and Weizhu Chen. Lora: Low-rank adaptation of large language models. *arXiv preprint arXiv:2106.09685*, 2021. [5](#)
- [22] Zhengyuan Jiang, Jinghuai Zhang, and Neil Zhenqiang Gong. Evading watermark based detection of ai-generated content. In *Proceedings of the 2023 ACM SIGSAC Conference on Computer and Communications Security*, pages 1168–1181, 2023. [1](#)
- [23] Diederik Kingma, Tim Salimans, Ben Poole, and Jonathan Ho. Variational diffusion models. *Advances in neural information processing systems*, 34:21696–21707, 2021. [2](#)
- [24] Satyam Kumar, Dayima Musharaf, Seerat Musharaf, and Anil Kumar Sagar. A comprehensive review of the latest advancements in large generative ai models. In *Advanced Communication and Intelligent Systems*, pages 90–103, Cham, 2023. Springer Nature Switzerland. [1](#)
- [25] Qiao Li, Xiaomeng Fu, Xi Wang, Jin Liu, Xingyu Gao, Jiao Dai, and Jizhong Han. Unveiling structural memorization: Structural membership inference attack for text-to-image diffusion models. In *Proceedings of the 32nd ACM International Conference on Multimedia*, pages 10554–10562, 2024. [1](#)
- [26] Xin Li, Yulin Ren, Xin Jin, Cuiling Lan, Xingrui Wang, Wenjun Zeng, Xinchao Wang, and Zhibo Chen. Diffusion

models for image restoration and enhancement – a comprehensive survey, 2023. 1

[27] Yiming Li, Yang Bai, Yong Jiang, Yong Yang, Shu-Tao Xia, and Bo Li. Untargeted backdoor watermark: Towards harmless and stealthy dataset copyright protection. *Advances in Neural Information Processing Systems*, 35:13238–13250, 2022. 1

[28] Yixin Liu, Chenrui Fan, Yutong Dai, Xun Chen, Pan Zhou, and Lichao Sun. Metacloak: Preventing unauthorized subject-driven text-to-image diffusion-based synthesis via meta-learning. In *Proceedings of the IEEE/CVF Conference on Computer Vision and Pattern Recognition*, pages 24219–24228, 2024. 3

[29] Ziwei Liu, Ping Luo, Xiaogang Wang, and Xiaou Tang. Deep learning face attributes in the wild. In *Proceedings of the IEEE international conference on computer vision*, pages 3730–3738, 2015. 5, 1

[30] Yawei Lu, Matthew Y. R. Yang, Zuoqiu Liu, Gautam Kamath, and Yaoliang Yu. Disguised copyright infringement of latent diffusion models, 2024. 1

[31] Nils Lukas, Abdulrahman Diaa, Lucas Fenaux, and Florian Kerschbaum. Leveraging optimization for adaptive attacks on image watermarks. In *The Twelfth International Conference on Learning Representations*, 2024. 1

[32] Ge Luo, Junqiang Huang, Manman Zhang, Zhenxing Qian, Sheng Li, and Xinpeng Zhang. Steal my artworks for finetuning? a watermarking framework for detecting art theft mimicry in text-to-image models, 2023. 1, 3, 5, 6

[33] Tomoya Matsumoto, Takayuki Miura, and Naoto Yanai. Membership inference attacks against diffusion models. In *2023 IEEE Security and Privacy Workshops (SPW)*, pages 77–83. IEEE, 2023. 1

[34] Chenlin Meng, Yutong He, Yang Song, Jiaming Song, Jiajun Wu, Jun-Yan Zhu, and Stefano Ermon. Sdedit: Guided image synthesis and editing with stochastic differential equations. In *International Conference on Learning Representations*, 2022. 5

[35] Taehong Moon, Moonseok Choi, Gayoung Lee, Jung-Woo Ha, and Juho Lee. Fine-tuning diffusion models with limited data. In *NeurIPS 2022 Workshop on Score-Based Methods*, 2022. 3

[36] Alex Nichol, Prafulla Dhariwal, Aditya Ramesh, Pranav Shyam, Pamela Mishkin, Bob McGrew, Ilya Sutskever, and Mark Chen. Glide: Towards photorealistic image generation and editing with text-guided diffusion models. *arXiv preprint arXiv:2112.10741*, 2021. 1

[37] Yan Pang and Tianhao Wang. Black-box membership inference attacks against fine-tuned diffusion models. *arXiv preprint arXiv:2312.08207*, 2023. 1

[38] Lorenzo Papa, Lorenzo Faiella, Luca Corvitto, Luca Maiano, and Irene Amerini. On the use of stable diffusion for creating realistic faces: from generation to detection. In *2023 11th International Workshop on Biometrics and Forensics (IWBF)*, pages 1–6, 2023. 2

[39] Justin N. M. Pinkney. Pokemon blip captions. <https://huggingface.co/datasets/lambdalabs/pokemon-blip-captions/>, 2022. 1

[40] Justin N. M. Pinkney. Pokemon blip captions. <https://huggingface.co/datasets/lambdalabs/pokemon-blip-captions/>, 2022. 5

[41] Aimon Rahman, Jeya Maria Jose Valanarasu, Ilker Haci-haliloglu, and Vishal M. Patel. Ambiguous medical image segmentation using diffusion models. In *Proceedings of the IEEE/CVF Conference on Computer Vision and Pattern Recognition (CVPR)*, pages 11536–11546, 2023. 1

[42] Aditya Ramesh, Mikhail Pavlov, Gabriel Goh, Scott Gray, Chelsea Voss, Alec Radford, Mark Chen, and Ilya Sutskever. Zero-shot text-to-image generation, 2021. 1

[43] Robin Rombach, Andreas Blattmann, Dominik Lorenz, Patrick Esser, and Björn Ommer. High-resolution image synthesis with latent diffusion models. In *Proceedings of the IEEE/CVF Conference on Computer Vision and Pattern Recognition (CVPR)*, pages 10684–10695, 2022. 1, 2, 4, 5

[44] Mehrdad Saberi, Vinu Sankar Sadasivan, Keivan Rezaei, Aounon Kumar, Atoosa Chegini, Wenxiao Wang, and Soheil Feizi. Robustness of ai-image detectors: Fundamental limits and practical attacks. In *The Twelfth International Conference on Learning Representations*, 2024. 1

[45] Chitwan Saharia, William Chan, Saurabh Saxena, Lala Li, Jay Whang, Emily L Denton, Kamyar Ghasemipour, Raphael Gontijo Lopes, Burcu Karagol Ayan, Tim Salimans, et al. Photorealistic text-to-image diffusion models with deep language understanding. *Advances in Neural Information Processing Systems*, 35:36479–36494, 2022. 2

[46] Christoph Schuhmann, Romain Beaumont, Richard Vencu, Cade Gordon, Ross Wightman, Mehdi Cherti, Theo Coombes, Aarush Katta, Clayton Mullis, Mitchell Wortsman, et al. Laion-5b: An open large-scale dataset for training next generation image-text models. *Advances in Neural Information Processing Systems*, 35:25278–25294, 2022. 1

[47] Shawn Shan, Jenna Cryan, Emily Wenger, Haitao Zheng, Rana Hanocka, and Ben Y Zhao. Glaze: Protecting artists from style mimicry by {Text-to-Image} models. In *32nd USENIX Security Symposium (USENIX Security 23)*, pages 2187–2204, 2023. 3

[48] Xudong Shen, Chao Du, Tianyu Pang, Min Lin, Yongkang Wong, and Mohan Kankanhalli. Finetuning text-to-image diffusion models for fairness. *arXiv preprint arXiv:2311.07604*, 2023. 3

[49] Reza Shokri, Marco Stronati, Congzheng Song, and Vitaly Shmatikov. Membership inference attacks against machine learning models. In *2017 IEEE symposium on security and privacy (SP)*, pages 3–18. IEEE, 2017. 1

[50] Gowthami Somepalli, Vasu Singla, Micah Goldblum, Jonas Geiping, and Tom Goldstein. Understanding and mitigating copying in diffusion models. *Advances in Neural Information Processing Systems*, 36:47783–47803, 2023. 1

[51] Diangarti Tariang, Riccardo Corvi, Davide Cozzolino, Giovanni Poggi, Koki Nagano, and Luisa Verdoliva. Synthetic image verification in the era of generative ai: What works and what isn't there yet, 2024. 1

[52] Thanh Van Le, Hao Phung, Thuan Hoang Nguyen, Quan Dao, Ngoc N Tran, and Anh Tran. Anti-dreambooth: Protecting users from personalized text-to-image synthesis. In

Proceedings of the IEEE/CVF International Conference on Computer Vision, pages 2116–2127, 2023. 3

- [53] Zhenting Wang, Chen Chen, Lingjuan Lyu, Dimitris N Metaxas, and Shiqing Ma. Diagnosis: Detecting unauthorized data usages in text-to-image diffusion models. In *The Twelfth International Conference on Learning Representations*, 2023. 1, 3, 5, 6
- [54] Xianchao Wu. Creative painting with latent diffusion models. In *Proceedings of the Second Workshop on When Creative AI Meets Conversational AI*, pages 59–80, Gyeongju, Republic of Korea, 2022. Association for Computational Linguistics. 1
- [55] Ling Yang, Zhilong Zhang, Yang Song, Shenda Hong, Runsheng Xu, Yue Zhao, Wentao Zhang, Bin Cui, and Ming-Hsuan Yang. Diffusion models: A comprehensive survey of methods and applications. *ACM Computing Surveys*, 56(4):1–39, 2023. 2
- [56] Tao Yang, Rongyuan Wu, Peiran Ren, Xuansong Xie, and Lei Zhang. Pixel-aware stable diffusion for realistic image super-resolution and personalized stylization, 2024. 1
- [57] Ning Yu, Vladislav Skripniuk, Sahar Abdelnabi, and Mario Fritz. Artificial fingerprinting for generative models: Rooting deepfake attribution in training data. In *Proceedings of the IEEE/CVF International conference on computer vision*, pages 14448–14457, 2021. 1, 3, 5, 6
- [58] Lvmin Zhang, Anyi Rao, and Maneesh Agrawala. Adding conditional control to text-to-image diffusion models. In *Proceedings of the IEEE/CVF International Conference on Computer Vision*, pages 3836–3847, 2023. 2
- [59] Yang Zhang, Teoh Tze Tzun, Lim Wei Hern, and Kenji Kawaguchi. On copyright risks of text-to-image diffusion models. In *ECCV 2024 Workshop The Dark Side of Generative AIs and Beyond*, 2024. 1
- [60] Xuandong Zhao, Kexun Zhang, Zihao Su, Saastha Vasan, Ilya Grishchenko, Christopher Kruegel, Giovanni Vigna, Yu-Xiang Wang, and Lei Li. Invisible image watermarks are provably removable using generative ai. *Advances in Neural Information Processing Systems*, 2024. 1

Exploiting Watermark-Based Defense Mechanisms in Text-to-Image Diffusion Models for Unauthorized Data Usage

Supplementary Material

7. Dataset Details

In this section, we provide more information about the datasets utilized in this work.

- Pokémon [39]: This dataset consists of 833 text-image pairs. The captions for the images were generated using the BLIP model.
- Naruto [7]: This dataset contains 1,121 text-image pairs. Similar to the Pokémon dataset, the captions were generated using the BLIP model.
- CelebA [29]: This dataset includes images of celebrities' faces paired with captions generated by the LLAVA model. While the full dataset contains 36,646 text-image pairs, we selected 1,000 pairs to ensure consistency with the experimental setup in DIAGNOSIS [53].

8. Evaluation on Different Models

The experiments in Section 5 of the main text are conducted on Stable Diffusion v1.4. In this section, we evaluate the efficacy of RATTAN against other popular models, including Stable Diffusion v2.0 and Stable Diffusion v2.1.

The results, reported in Table 4, demonstrate that DIAGNOSIS successfully embeds watermarks across all models with a detection rate over 95%. However, it is not resilient to RATTAN, which effectively removes the watermark from every model. RATTAN achieves a 100% evasion of detection on watermarked models by DIAGNOSIS, converting all true positives into false negatives while leaving benign models unaffected.

The results demonstrate that RATTAN's performance is consistent across various text-to-image models, showing no degradation in its ability to mitigate watermarks, regardless of the model architecture or version differences. RATTAN not only removes watermarks but also ensures that the benign attributes of the models remain unaffected.

9. Visualizations

In this section, we present visualizations of images generated during the controlled generation process of RATTAN, along with visualizations of images produced by the trained text-to-image models.

9.1. Controlled Generation Diffusion Process

RATTAN utilizes the diffusion process to generate a new image based on the original protected image and its corresponding text. This process involves several steps to progressively denoise the added Gaussian noise. We use 60

steps as the default setting and show the intermediate images produced during this process. The results are illustrated in Figure 4 and Figure 5, with $\gamma = 0.6$ and $\gamma = 1.0$, respectively.

With $\gamma = 0.6$, noise is not added to the original protected image until it fully becomes Gaussian noise; instead, the process is stopped at 60% of the noise-adding stage, as discussed in Section 4.2. From Figure 4(b), it can be observed that the image retains the high-level key features of the protected input shown in (a). The artifacts from the watermark are largely removed by the introduced noise. The subsequent denoising steps gradually refine the image's details, culminating in the final output in (f). The final image retains all the key features of the watermarked input in (a) but is free from the watermark.

Figure 5 illustrates the intermediate results with a higher γ value. The stronger noise significantly obscures the high-level features, as seen in (b). As a result, the subsequent denoising process struggles to retain these features, instead generating an image primarily based on the model's inherent generation capabilities. In the final output, shown in (f), the features are very different from those in (a), and the generated image no longer resembles the original input. Therefore, a smaller γ is preferred in RATTAN to preserve the main features better.

9.2. Effect of γ

In this section, we visually examine the controlled generation results using various γ values tested in the ablation study presented in the main paper. Figure 6 displays the images generated with different parameters, demonstrating the influence of γ on output quality and the effectiveness of watermark removal.

As expected, increasing the γ value introduces more noise into the initial input image, leading to a more significant divergence from the original input. This effect is particularly evident in our results, especially in (e) and (f), where the images exhibit significant degradation and divergence from the original watermarked input image (a). Consequently, models trained with these settings tend to have a higher FID score (indicating lower generated image quality), as reported in Table 3 in the main text.

On the other hand, a smaller γ value ensures that the controlled generation closely follows the original input, thereby preserving high-level features. However, this also means that watermark artifacts are retained, as shown in (b) and (c). Models trained on these generated images can still be

Table 4. Evaluation of RATTAN against DIAGNOSIS on the Pokemon dataset with different Stable Diffusion models.

Model	Method	Metrics					FID \downarrow	Memorization \downarrow
		TP	TN	FP	FN	Acc		
Stable Diffusion v1.4	DIAGNOSIS	10	10	0	0	100%	214.86 ± 9.02	0.830
	RATTAN	0	10	0	10	50%	211.59 ± 3.15	0.327
Stable Diffusion v2.0	DIAGNOSIS	10	10	0	0	100%	241.12 ± 6.82	0.952
	RATTAN	0	10	0	10	50%	242.66 ± 13.96	0.444
Stable Diffusion v2.1	DIAGNOSIS	9	10	0	1	95%	236.01 ± 9.46	0.872
	RATTAN	0	10	0	10	50%	240.44 ± 9.06	0.378

detected with the watermark, as also noted in [Table 3](#).

We find that $\gamma = 0.6$ achieves an optimal balance between mitigating the watermark and retaining the key features of the original input image.

9.3. Generated Images

In this section, we present examples of images generated under three scenarios: a benign model fine-tuned on the Pokémon dataset without any watermarks, a watermarked model produced by DIAGNOSIS, and a watermark-removed model by RATTAN.

The results are presented in [Figure 7](#). The first row displays images generated by a benign model. The second and third rows show images generated by DIAGNOSIS-watermarked models using an unconditional watermark and a trigger-conditioned watermark, respectively. The final two rows depict images generated by watermark-cleaned models from RATTAN. The results show minimal visual quality loss in the images between DIAGNOSIS and RATTAN. Most images successfully reproduce similar subjects, retaining key attributes such as colors, creature types, and positioning within the image. This highlights that RATTAN effectively removes watermarks without compromising the generative performance of cleaned models. These findings indicate that RATTAN effectively targets and removes watermark-related artifacts while preserving the underlying image distribution. This ensures that the model’s utility remains intact for the adversary, enabling it to generate content in the style of copyrighted material without facing the associated consequences. This underscores the critical need for developing more robust and effective methods to protect intellectual property and private data.

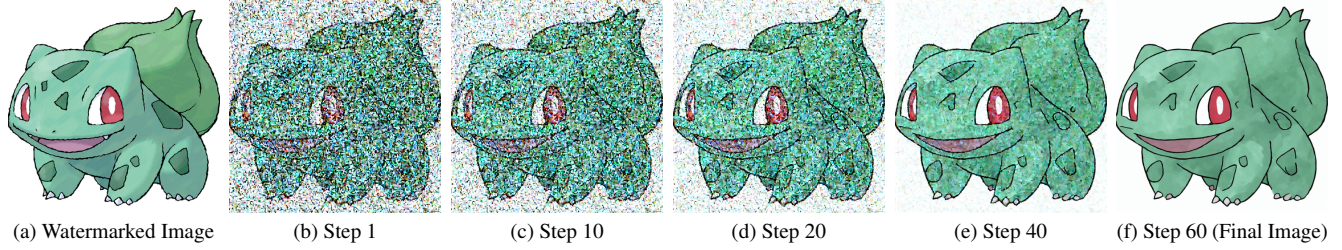


Figure 4. Intermediate images during controlled image generation of RATTAN with $\gamma = 0.6$.

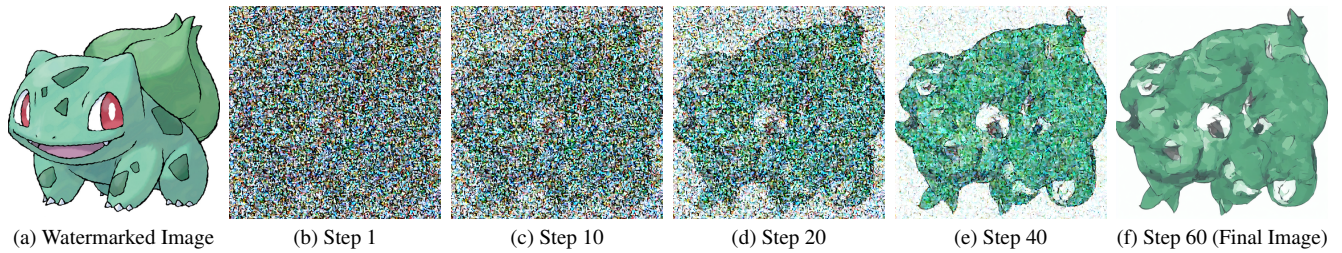


Figure 5. Intermediate images during controlled image generation of RATTAN with $\gamma = 1.0$.

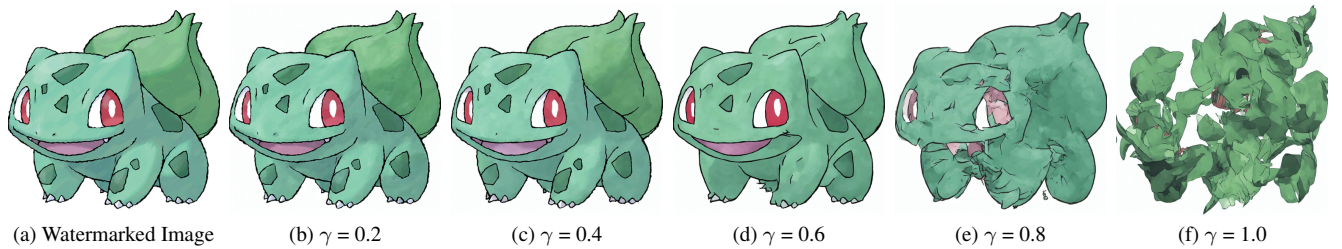


Figure 6. Effect of γ on RATTAN's controlled generation process.

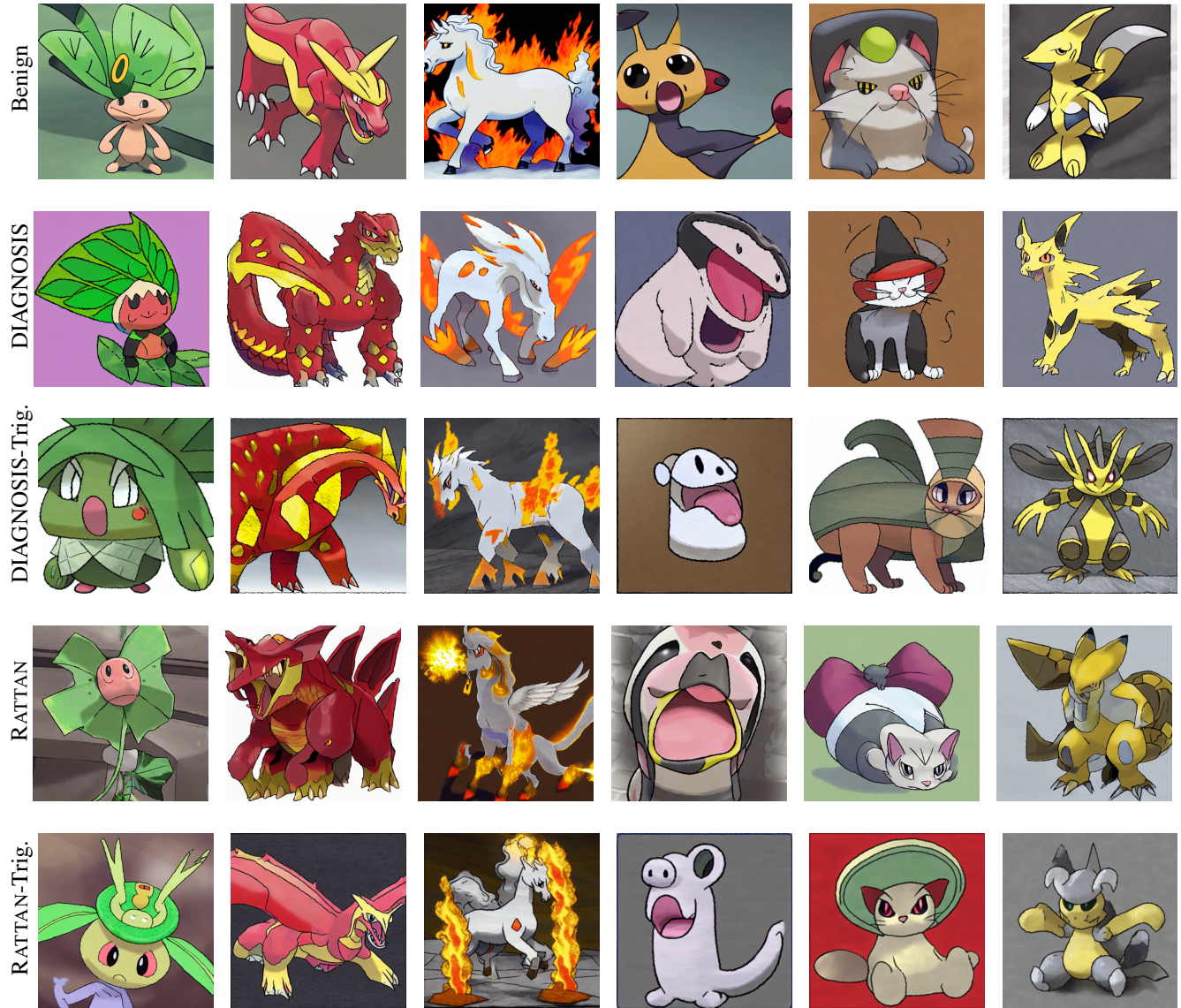


Figure 7. Generated images from the benign model, DIAGNOSIS-watermarked model, and RATTAN-cleaned model. Trig. refers to the use of a trigger-conditioned watermark.